Geomechanics and Engineering, *Vol. 41, No. 6 (2025) 597-609*
https://doi.org/10.12989/gae.2025.41.6.597

Sustainable stabilization of soft soils through reactive MgO-$MgCl_2$ carbonation: Mechanistic insights and performance optimization

Guanghua Cai*[1], Yibo Wang[1], Zhaoyuan Guo[2,4], Han Zhang[1], Tianyun Liu[3], Hongsen Liu[5] and Chi-Sun Poon[6]

[1]*College of Civil and Engineering, Nanjing Forestry University, Nanjing 210037, China*
[2]*School of Transportation, Southeast University, Nanjing 211189, China*
[3]*Tianjin Port Engineering Institute Ltd. of CCCC First Harbor Engineering Company Ltd., Tianjin 300222, China*
[4]*Jiangsu Provincial Transportation Engineering Construction Bureau, Nanjing 210004, China*
[5]*Yellow River Engineering Consulting Co., LTD, Zhengzhou 450003, China*
[6]*Department of Civil and Environmental Engineering, The Hong Kong Polytechnic University, Kowloon, Hong Kong*

(*Received March 21, 2025, Revised May 28, 2025, Accepted June 4, 2025*)

Abstract. Portland cement, a conventional binder for soft soil stabilization, faces limitations in treating specialized soils due to its high carbon footprint and environmental impact during production. This study proposed an eco-friendly alternative using reactive magnesia (MgO) and magnesium chloride ($MgCl_2$) for carbonation treatment of saline soft soils. The mechanical properties, hydrochemical behavior, water stability, and microstructural evolution of carbonation-stabilized soils were systematically investigated under varying salinity levels ($MgCl_2$ content) and initial moisture conditions. Key findings revealed that unconfined compressive strength and modulus decreased with increasing initial water content but exhibited a unique trend under $MgCl_2$ variation—initial gradual reduction (3–6% $MgCl_2$) followed by significant enhancement (6–12% $MgCl_2$). Carbonation efficiency declined from 40% to 10% with rising initial water content, while showing a V-shaped relationship with $MgCl_2$ dosage (minimum at 6%). Post-carbonation pH decreased with higher $MgCl_2$ content and lower initial moisture, whereas electrical conductivity increased proportionally to both parameters. Microstructural analyses identified distinct phase formations: low-$MgCl_2$ (6%) systems produced flower-like hydromagnesite, spheroidal dypingite, and prismatic nesquehonite, while high-$MgCl_2$ (12%) systems generated short-rod chloro-carbonates and acicular magnesium oxychloride crystals ($5Mg(OH)_2 \cdot MgCl_2 \cdot 8H_2O$). These crystalline phases collectively enhanced soil stabilization. Optimized performance was achieved at a magnesium-chloride molar ratio <6 and a water-chloride ratio of 12–17, demonstrating the viability of MgO-$MgCl_2$ carbonation activation for sustainable soil stabilization.

Keywords: carbonation stabilization; engineering properties; magnesium chloride; microstructural characterization reactive MgO

1. Introduction

Chloride-laden saline soils present significant geotechnical challenges including foundation immersion collapse, frost heave, thaw settlement, and reinforced concrete corrosion (Liu *et al*. 2021, Gao *et al*. 2011). The aggressive nature of chloride ions induces concrete pile cracking and steel reinforcement deterioration, ultimately compromising structural integrity (Zhang *et al.* 2014) These risks necessitate soil stabilization before foundation construction. While chemical stabilization remains prevalent due to its operational simplicity, rapid implementation, and cost-effectiveness (Sun *et al*. 2014), conventional Portland cement (PC) - the most common chemical stabilizer - faces two critical limitations: (a) substantial carbon footprint from production processes accounting for 5-7% of global anthropogenic CO_2 emissions (Miller and Moore 2020) and (b) performance degradation in saline environments (Yang *et al*. 2014). The instability of PC-treated saline soils stems from detrimental interactions between cement hydration products and salt ions. Sulfates worsen this issue by reacting with calcium-based materials to form expansive minerals like ettringite, reducing structural stability (Sagidullina *et al*. 2025). Chlorides chemically react with Ca^{2+} in cemented soils, destabilizing cementitious matrices (Yu 2004). Concurrently, mobile Mg^{2+} ions penetrate cement structures, reacting with calcium silicate hydrates (C-S-H) to form weakly cementitious magnesium silicate hydrates while inducing crack formation (Zhao *et al.* 2020). Engineering practice reveals that magnesium salt-load coupling effects would accelerate the deterioration of cemented soil, with decomposing into porous brucite ($Mg(OH)_2$) with consequent strength reduction (He *et al*. 2017). Emerging reactive MgO carbonation technology addressed this limitation while offering environmental advantages over PC stabilization (Li *et al*. 2023, 2024, Onyekwena *et al.* 2023). This innovative approach enabled rapid soil improvement through CO_2 sequestration, achieving porosity reduction and strength enhancement within several hours (Cai *et al.* 2017, 2020, Seo *et al*. 2024). Carbonation converted MOC

*Corresponding author, Associate Professor
E-mail: ghcai@njfu.edu.cn

ISSN: 2005-307X (Print), 2092-6219 (Online)

Table 1 Physical and chemical properties of soil and reactive MgO

Property	Index value	
	Silty clay	MgO
Natural water content, w/%	29.2	--
Liquid limit, w_L/%	41.4	--
Plastic limit, w_P/%	20.7	--
Plasticity index	20.7	--
Relative density, Gs	2.67	2.25
pH	7.85	--
Grain-size distribution (%)		
Clay (< 0.005 mm)	17.4	73.5
Silt (0.005-0.075 mm)	69.4	26.5
Sand (0.075-20)	13.2	0

hydration products into low-solubility stable chloride-carbonate phases ($Mg_2CO_3(OH)Cl{\cdot}2\text{-}3H_2O$), simultaneously improving mechanical performance and water resistance (Ma *et al*. 2010). In addition, previous studies have shown that calcium silicate hydrate gel and layered double hydroxide are formed during the carbonation of MgO (Wang *et al.* 2024). Recent studies have demonstrated the enhancement of aqueous stability in cementitious materials through carbonation mechanisms. Walling and Provis (2016) systematically investigated the carbonation process, revealing that both triphasic and pentaphasic products exhibited significantly improved water resistance under carbonation conditions while elucidating the underlying reaction pathways.

Complementary to these findings, Góchez *et al*. (2017) reported that a reactive mixture of magnesium oxide (MgO) and magnesium chloride ($MgCl_2$) in aqueous media underwent carbonation in CO_2-rich environments, resulting in the formation of insoluble magnesium carbonate films that effectively enhanced the hydrological stability of magnesium salts exhibiting greater corrosive potential than sodium salts (Aye and Oguchi 2011). These dual mechanisms of chloride and magnesium interference significantly impede PC hydration, rendering conventional cement stabilization ineffective for saline soils. This necessitates the urgent development of low-carbon alternative binders specifically engineered for saline soil stabilization.

Recent advancements have highlighted magnesium oxychloride cement (MOC) as a promising eco-friendly alternative, formed through MgO-$MgCl_2$ reactions in humid environments. Initial studies demonstrated MOC's ability to generate high-strength, corrosion-resistant triphasic and pentaphasic hydration products ($3Mg(OH)_2{\cdot}MgCl_2{\cdot}8H_2O$ and $5Mg(OH)_2{\cdot}MgCl_2{\cdot}8H_2O$), suggesting its potential for saline soil stabilization (Karimi and Monshi 2011). However, these phases exhibited poor water stability, readily cement-based composites.

Despite these advancements, there were critical knowledge gaps regarding the effects of $MgCl_2$ concentration and initial moisture content on the physicochemical and mechanical properties of MOC-carbonated soils. Although preliminary studies have verified the feasibility of magnesium oxychloride cement (MOC) and reactive MgO carbonation technology, there are still some limitations:

- Existing research has mostly focused on MgO sand mixtures or artificially synthesized soils, lacking systematic exploration of the synergistic mechanism of hydration and carbonation in saline soft clay;
- The quantitative relationship between $MgCl_2$ dosage and carbonation efficiency lacks systematic research, and the interactive effects of $MgCl_2$ concentration and initial moisture content on carbonation efficiency and phase transition pathway have not been clarified, resulting in a lack of theoretical support for the optimization of engineering parameter;
- The microstructure evolution mechanism during carbonation process is still unclear, and the quantitative relationship between the water-immersion durability enhancement mechanism of MOC carbonation products (such as the formation of chlorocarbonate phase) and mechanical properties is still unclear, which restricts the promotion of technology.

The above limitations hinder the engineering application of MgO-$MgCl_2$ carbonation technology, and there is an urgent need to fill the knowledge gap through multi-scale research.

Therefore, this study systematically investigated the synergistic application of reactive MgO and $MgCl_2$ for the carbonation stabilization of saline soil. Through comprehensive testing encompassing unconfined compressive strength, carbonation rate, moisture content, pH, and conductivity measurements, treatment effectiveness was evaluated under varying $MgCl_2$ concentrations and initial moisture contents. Fundamental improvement mechanisms were revealed at microstructural and phase transformation levels through advanced microanalytical techniques including X-ray diffraction (XRD), scanning electron microscopy (SEM), and thermogravimetry (TGA). The findings will advance the practical implementation of

Table 2 Main chemical compositions of experimental materials (%)

Composition	Sample	MgO
MgO	1.22	95.2
Al_2O_3	10.22	0.42
CaO	6.41	0.46
SiO_2	71.76	1.58
Fe_2O_3	3.57	0.3
SO_3	0.27	0.1
K_2O	3.67	0.01

Table 3 Test scheme under different conditions

Water content *W*/%	$MgCl_2$ content *M*/%	Sample number
25	0、3、6、9、12	$W_{25}M_0$、$W_{25}M_3$、$W_{25}M_6$、$W_{25}M_9$、$W_{25}M_{12}$
30		$W_{30}M_0$、$W_{30}M_3$、$W_{30}M_6$、$W_{30}M_9$、$W_{30}M_{12}$
35		$W_{35}M_0$、$W_{35}M_3$、$W_{35}M_6$、$W_{35}M_9$、$W_{35}M_{12}$

MgO-$MgCl_2$ carbonation technology for the stabilization of saline soil while contributing theoretical insights for sustainable geotechnical engineering and carbon sequestration strategies.

2. Materials and methods

2.1 Materials

The soil utilized in this investigation was collected from the construction site of the foundation pit project of Mozhou East Road in Nanjing. This soil was classified as low-liquid-limit silty clay based on its physical and chemical properties, which were determined following the *Highway Geotechnical Test Procedure* (JTG 3430-2020). The test results, including key parameters such as liquid limit, plastic limit, and particle size distribution, are summarized in Table 1. Magnesia (MgO) employed in the experiments was a low-activity construction-grade material, while magnesium chloride ($MgCl_2$) consisted of industrial-grade powder. Both MgO and anhydrous $MgCl_2$ were procured from a magnesium manufacturing company in Dashiqiao, China. The MgO exhibited an activity index and purity of 65.8 and 95.2%, with a specific surface area of 7.22 m^2/g and a mean pore diameter of 49.6 nm. Chemical compositions of soil and MgO were analyzed using an X-ray fluorescence spectrometer (XRF), and the detailed results are presented in Table 2.

The soil selected in this study is silty clay from Nanjing, which has typical saline soil characteristics. The clay content is 17.4%, the plasticity index is 20.7, and the natural Cl- content is 0.5%~2%, representing the widely distributed soft soil types in China's eastern coastal and Yangtze River Delta regions, as per the "*Code for investigation of geotechnical engineering* (GB 50021-2001)". While there are regional differences in the mineral composition of saline soils worldwide--such as montmorillonite-dominated clay in the Nile Delta and silty soils along the U.S. Gulf Coast--their common traits of high salinity (Cl- 0.5%~15%), low permeability, and high expansibility are highly similar to the soil samples in this study (Li 2016). Thus, our findings offer a meaningful theoretical reference for similar saline soil and soft soil areas globally.

2.2 Methods

The experimental design incorporated chloride salt concentrations ranging from 0% to 12% by the weight ratio of dry soil, which aligns with typical chloride levels (0.5–15%) observed in high-salinity regions of China (Wan 2022). This range accounts for both natural chloride content in saline soils and the supplementary $MgCl_2$ introduced as part of the binder system. Initial water content, a critical factor influencing carbonation efficiency, was set at 25%, 30%, and 35% based on prior research by Cai *et al*. (2017, 2020). Reactive referring to the research findings of Jun *et al.* (2024), the carbonation reaction efficiency was optimized by adjusting the active MgO content. In this study, the active MgO content was set at 15% (based on dry soil mass ratio), CO_2 ventilation pressure is 100 kPa, ventilation time is 12 hours. Specimens were systematically labeled using the format "W_iM_j", where W_i denotes the initial water content (i=25%, 30%, and 35%) and M_j represents the $MgCl_2$ content (j=0, 3%, 6%, 9%, and 12%). The full factorial experimental matrix is detailed in Table 3.

2.3 Sample preparation and carbonization

Soil samples were air-dried, homogenized, and sieved through a 1.0 mm geotechnical sieve by the *Standard for Geotechnical Test Methods* (GB/T 50123-2019). Dry soil, MgO, and $MgCl_2$ were precisely weighed according to predetermined ratios and mechanically blended to achieve uniform distribution.

Deionized water was added to the dry mixture. The pre-weighed amount of deionized water was gradually added to the dry mixture while maintaining continuous agitation using a mechanical mixer. To mitigate heat generation from the exothermic hydration reactions of MgO and $MgCl_2$, the mixture was cooled to ambient temperature (~25°C) for 10 min before compaction. The homogenized mixture was statically compacted into cylindrical molds (50 mm diameter × 50 mm height) in three successive layers to achieve a target density of 1.88 g/cm^3. Molded specimens were cured for 24 hours under controlled conditions (23±2ºC, ≥95% relative humidity) to facilitate initial hydration and strength development.

Post-curing specimens were demoulded, dimensionally tested, and positioned on 2 mm aperture metal sieves within a pressurized carbonation chamber (Fig. 1). The chamber was initially purged with CO_2 at 20 kPa for 2 min to evacuate residual air, followed by pressurization to 100 kPa

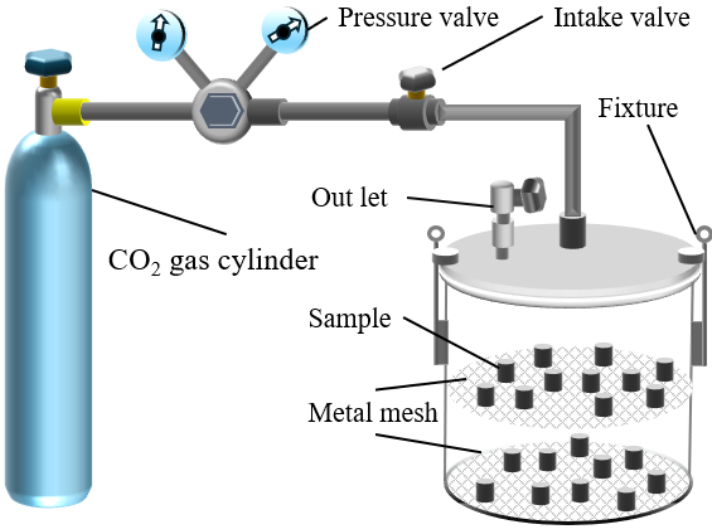

Fig. 1 Diagram of carbonation device

for sustained carbonation over 12 hours. To maximize CO_2 utilization, the system remained sealed for an additional 12 hours post-injection, allowing gradual pressure decay while maintaining carbonation reactivity. Specimens were subsequently extracted, weighed, and dimensionally re-measured to quantify carbonation-induced mass changes.

2.4 Experimental procedure

Carbonation efficiency was evaluated using the actual carbon uptake ratio (S_{car}), calculated as

$$S_{car} = \frac{m_2 - m_1}{m_{MgO}} \times 100\% \quad (1)$$

Where m_1 and m_2 represent the mass of the pre- and post- carbonation respectively (g); and m_{MgO} denotes the MgO mass in the sample (g). This metric assumes a theoretical 1:1 molar ratio between MgO and CO_2 during complete carbonation, corresponding to a mass ratio of 0.8-1.1 (Cai *et al*. 2017).

Unconfined compressive strength (UCS) tests were conducted using a WDT-100B strain-controlled compression tester at a displacement rate of 1 mm/min. Post-test fragments were analyzed for moisture content via oven-drying at 45°C to prevent thermal decomposition of carbonation products. Next, the dried samples were ground, and then used for preparing soil-water suspensions (water-soil ratio of 2:1) for chemical characterization. The suspensions were agitated intermittently over 6 hours, followed by 2-hour sedimentation. Supernatant pH and conductivity were measured using an AS218 pH meter and DDS-11A conductivity meter, respectively, with triplicate measurements ensuring <10% variability. Under the error of less than 10%, the average value of three parallel tests was taken as the final result.

Microstructural analyses involved freeze-dried fresh specimen fragments in liquid nitrogen (-80ºC, >8 hours) using a GOLD-SIM FD5 lyophilizer. Surface morphology was examined via FEI Quanta 2000 SEM at ×1500 magnification after gold sputtering. The composition was characterized by X-ray diffraction (Rigaku SmartLab, Cu-Kα radiation, 3 kW, 5–65° 2θ range, 0.02° step size, 10°/min) and thermogravimetric analysis (NETZSCH TG 209F3, N_2 atmosphere, 30–850°C, 5°C/min). All ground samples passed through a 75 μm sieve before XRD and TGA instrumental analysis.

3. Results and discussion

3.1 Mechanical properties

Mechanical properties, including unconfined compressive strength (UCS) and deformation modulus (E_{50}), are vital for evaluating the usability of foundation soil in soil engineering. Subsequent research focuses on UCS and E_{50} of carbonated/solidified soil to comprehensively evaluate the macroscopic mechanical properties of MgO-$MgCl_2$ carbonated solidified soil.

3.1.1 Unconfined compressive strength

Fig. 2 demonstrates the variation of unconfined compressive strength (UCS) in carbonation-solidified samples under varying initial moisture contents (25-35%) and $MgCl_2$ concentrations (0-9%). Three distinct behavioral patterns emerge: 1) at constant moisture content, UCS exhibits a characteristic V-shaped trend with $MgCl_2$ concentration - initially declining from 4.2 MPa (0% $MgCl_2$) to a minimum of 0.5 MPa (3-6% $MgCl_2$), followed by a marked recovery to peak strength (7.13 MPa at 9% $MgCl_2$); 2) under fixed $MgCl_2$ concentration, UCS shows progressive reduction with increasing moisture from 25% to 35%; and 3) moisture sensitivity becomes significantly more pronounced when $MgCl_2$ exceeds 6%, suggesting a shift in dominant reaction mechanisms.

The mechanical strength of carbonated/stabilized soil arises from the synergistic interaction between MgO carbonation and

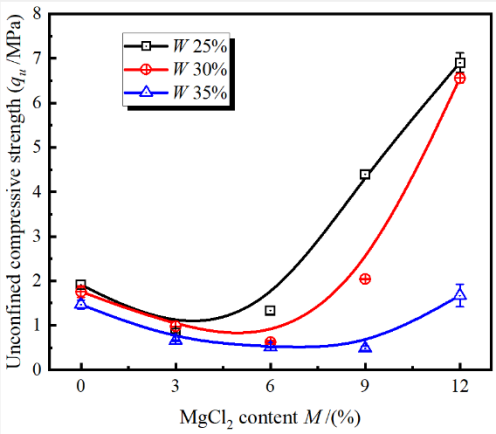

Fig. 2 Unconfined compressive strength under the varying $MgCl_2$ content

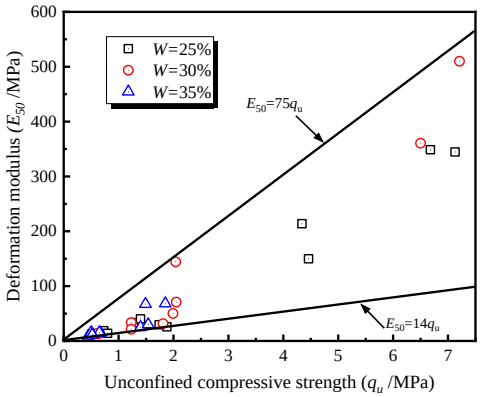

Fig. 3 The relationship between E_{50} and q_u of carbonized samples

Table 4 Calculation results of deformation modulus (E_{50})

$MgCl_2$ content/%	Water content /%		
	25	30	35
0	27.62	40.79	27.53
3	16.33	27.33	15.15
6	36.89	13.63	14.20
9	181.79	107.44	10.43
12	346.69	435.27	67.69

MgO-$MgCl_2$-H_2O (MOC) hydration reactions. Below 6% $MgCl_2$ concentration, the strength enhancement primarily derives from carbonate products formed through reactive MgO carbonation. When $MgCl_2$ exceeds 6% at moderate moisture levels (25-30%), strength development is predominantly governed by tri- and penta-phase hydration products from the MgO-$MgCl_2$-H_2O system. While these hydration products enable rapid particle bonding, their limited water stability explains the strength reduction observed at 35% moisture content (He *et al.* 2017). At the transitional 6% $MgCl_2$ concentration, both MOC hydration and MgO carbonation occur simultaneously. However, the suboptimal $MgCl_2$: MgO ratio inhibits the substantial formation of MOC hydration products. Concurrently, MgO consumption and pore structure refinement collectively reduce carbonate products. Furthermore, the elevated moisture content adversely affects the stability of tri-/penta-phase products while potentially impeding CO_2 diffusion, thereby diminishing the carbonation efficiency in MgO-stabilized soils (Liu *et al.* 2017). Optimal saline soil improvement through active MgO-CO_2 carbonation technology occurs when moisture content remains ≤30% combined with $MgCl_2$ concentrations >6% (Huang *et al.* 2022). This aligns with findings from MgO-CaO-FA blends, where peak strength was achieved at 6 hours of carbonation, followed by a plateau in reaction efficiency (Wang *et al.* 2019). This balanced condition promotes favorable reaction pathways while maintaining adequate carbonation efficiency and hydration product stability.

3.1.2 Deformation modulus

The deformation modulus (E_{50}) serves as the primary mechanical parameter characterizing soil resistance to deformation. Based on stress-strain curves obtained from unconfined compression tests, the deformation modulus was calculated using Eq. (2), with computational results presented in Table 4.

$$E_{50} = \frac{2\sigma_{1/2}}{\varepsilon_f} \tag{2}$$

where ε_f is the failure strain (%) corresponding to the peak stress; $\sigma_{1/2}$ is the axial stress (MPa) at 50% of failure strain.

Table 4 reveals that the deformation modulus E_{50} exhibits an initial decrease followed by a subsequent increase with rising $MgCl_2$ content while demonstrating an inverse relationship with initial moisture content - a trend consistent with UCS variations. Notably, when moisture content remains below 35% coupled with $MgCl_2$ concentrations exceeding 6%, a marked enhancement in deformation modulus occurs. However, the samples with a moisture content of 35% display significantly reduced moduli. This behavior can be attributed to moisture-induced inhibition of reactive MgO carbonation under high hydration conditions, where excess water compromises the stability of hydration products from MOC. Consequently, this degradation reduces effective bonding between hydration products and soil particles, ultimately diminishing the specimen's deformation resistance.

Fig. 3 illustrates the correlation between deformation modulus and UCS for MgO-$MgCl_2$ carbonated/stabilized soils. The plotted data demonstrates proportional growth of deformation moduli with strength development, forming a characteristic triangular distribution pattern that can be mathematically described by Eq. (3). These findings align with established research indicating a linear relationship between deformation moduli and UCS (Cai *et al.* 2015), particularly corroborating the conclusions regarding cemented soil behavior from Zhang *et al.* (2022).

$$E_{50} = (14 \sim 75)\, q_u \tag{3}$$

3.2 Physical and chemical properties

The physical and chemical properties of the samples, including carbon absorption rate, moisture content, pH value, and conductivity, serve as key indicators for

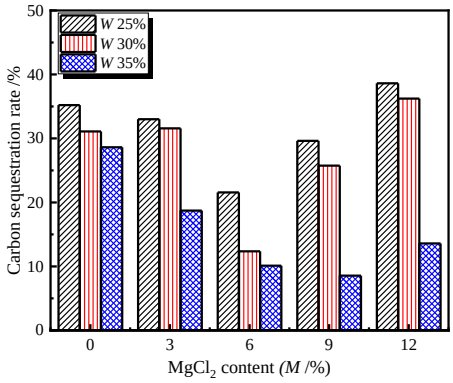

Fig. 4 Carbon absorption rate of samples

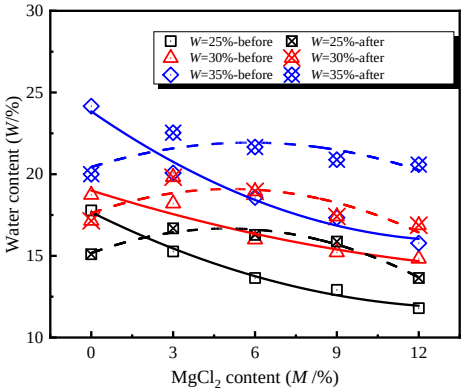

Fig. 5 Moisture content of sample before and after carbonation

carbonated/solidified soil. These properties provide theoretical support for revealing the strength formation mechanism of carbonated/solidified soil through subsequent micro experiments.

3.2.1 Carbon absorption rate

The carbon absorption rate quantifies the CO_2 sequestration capacity and reflects the carbonation degree of MgO-$MgCl_2$ carbonated/solidified soil specimens. Fig. 4 illustrates the variations in carbon absorption rate under different initial water contents and $MgCl_2$ concentrations, as calculated using Eq. (1). Experimental results reveal that carbon absorption rates range between 10% and 40%, exhibiting distinct trends. Absorption decreases systematically with increasing initial water content while showing a nonlinear relationship with $MgCl_2$ concentration characterized by an initial decline followed by recovery, reaching its minimum at 6% $MgCl_2$ content. This pattern aligns closely with the observed strength variations in specimens. Notably, the measured absorption rates are substantially lower than the theoretical range of 0.88–1.1 reported for fully carbonated MgO-sand systems (Yi *et al.* 2013), indicating incomplete carbonation of MgO in the current study. Four contributing factors are identified: (1) the clay particles in the soil matrix create diffusion barriers that hinder CO_2 infiltration and carbonation; (2) the relatively low activity of the MgO used reduces carbonation efficiency; (3) competitive chemical reactions between reactive MgO and $MgCl_2$ consume some MgO that would otherwise participate in carbonation; and (4) unfavorable high moisture conditions combined with 6% $MgCl_2$ concentration further suppress carbonation, ultimately compromising specimen strength.

3.2.2 Water content

Fig. 5 compares water content variations in specimens under different $MgCl_2$ concentrations and initial water contents before and after carbonation. Before carbonation, water content decreases progressively with increasing $MgCl_2$ concentration, a phenomenon attributed to water dissipation during the exothermic hydration reactions between $MgCl_2$ and water. Compared to the pre-carbonation samples, the post-carbonation samples exhibit elevated moisture content, which is attributed to the hygroscopicity of $MgCl_2$ during the carbonation process. Notably, at the 6% $MgCl_2$ content, the moisture content of carbonated samples increases sharply, coinciding with the minimum carbon absorption rate observed. This is likely due to the preferential hydration reaction between MgO and $MgCl_2$ at this $MgCl_2$ concentration, depleting MgO availability for carbonation. The combined effects of hydration product formation and $MgCl_2$ hygroscopicity further amplify moisture retention. These findings shed light on the mechanism by which excessive $MgCl_2$ reduces carbonation efficiency.

3.2.3 pH Value

Fig. 6 presents pH evolution in pore fluids under varying $MgCl_2$ concentrations and initial water contents. Pre-carbonation analysis demonstrates decreasing pH with higher $MgCl_2$ concentrations due to the acidic nature of $MgCl_2$ solutions (pH =~6.04) while increasing initial water content elevates pH through enhanced MgO hydration that releases OH^- ions (Eq. (4)) (Cai 2017). Post-carbonation specimens universally exhibit pH reduction compared to pre-carbonized states, though the pH declining rate diminishes with increasing $MgCl_2$ content and initial water content. This behavior reflects competing chemical pathways: carbonation consumes water during MgO conversion to carbonates (Eqs. (5)-(7)), lowering pH (Li *et al.* 2023), while concurrent MgO-$MgCl_2$ interactions generate alkaline byproducts (Eqs. (8) and (9)) (Sun *et al.* 2023). Threshold analysis reveals a critical $MgCl_2$ concentration boundary at 6%. Carbonation dominates chemistry reactions in specimens below this threshold, whereas hydration reactions prevail at $MgCl_2$ concentrations of more than 9%.

$$MgO+H_2O \rightarrow Mg(OH)_2 \rightarrow 2OH^-+Mg^2 \quad (4)$$

$$Mg(OH)_2+CO_2+2H_2O \rightarrow MgCO_3 \cdot 3H_2O \quad (5)$$

$$5Mg(OH)_2+4CO_2+4H_2O \rightarrow Mg_5(CO_3)_4(OH)_2 \cdot 5H_2O \quad (6)$$

$$5Mg(OH)_2+4CO_2 \rightarrow Mg_5(CO_3)_4(OH)_2 \cdot 4H_2O \quad (7)$$

$$4Mg^{2+}+2C1^-+6OH^-+8H_2O \rightarrow 3Mg(OH)_2 \cdot MgCl_2 \cdot 8H_2O \quad (8)$$

$$6Mg^{2+}+2C1^-+10OH^-+8H_2O \rightarrow 5Mg(OH)_2 \cdot MgCl_2 \cdot 8H_2O \quad (9)$$

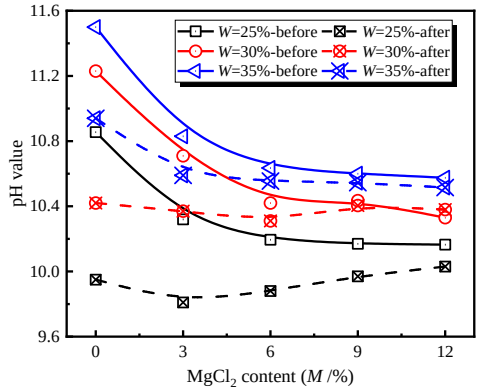

Fig. 6 pH value of samples before and after carbonation

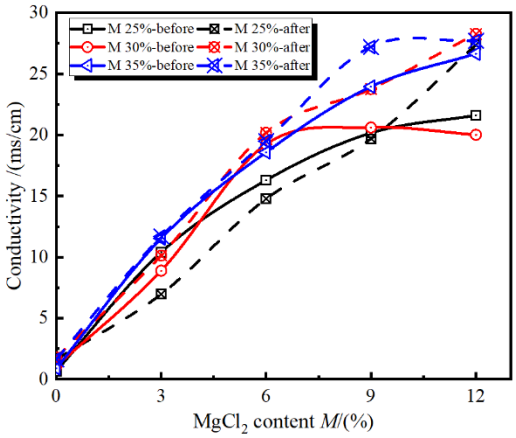

Fig. 7 Conductivity under varying $MgCl_2$ content and initial water content

3.2.4 Conductivity

Conductivity variations under different $MgCl_2$ concentrations and initial water contents are shown in Fig. 7. Both pre-carbonation and post-carbonation specimens demonstrate conductivity increases proportional to $MgCl_2$ concentration and initial water content. Conductivity exhibits a significant increase for post-carbonization specimens, measuring 7–26 times higher than $MgCl_2$-free counterparts. Three mechanisms drive this behavior: (1) $MgCl_2$'s strong electrolyte properties promote extensive ionization in aqueous phases; (2) elevated water content accelerates hydrolysis of both $MgCl_2$ and MgO, increasing ion mobility; and (3) carbonation has a minimal effect on cation concentration and salt content, preserving ionic strength. These findings confirm that conductivity enhancement primarily stems from $MgCl_2$'s electrolytic contributions rather than carbonation-induced chemical changes.

3.3 Microstructure analysis

To explore the micro improvement mechanism of MgO-$MgCl_2$ carbonated/solidified samples, this study employs X-ray diffraction (XRD), thermogravimetric/derivative thermogravimetric analysis (TG/DTG), and scanning electron microscopy (SEM) systems to analyze the phase composition, thermal decomposition characteristics, and microstructure of carbonation products. This approach aims to investigate the correlation between microstructure densification and macroscopic mechanical properties.

3.3.1 XRD analysis

The X-ray diffraction patterns of soil samples under varying $MgCl_2$ contents and initial water contents are presented in Figs. 8(a) and 8(b). The XRD analysis revealed the presence of multiple reaction products beyond conventional SiO_2 and kaolinite (K) peaks, including $Mg(OH)_2$, $MgCl_2$, various magnesium alkaline carbonates (labeled as N, D/H, L, and A with corresponding chemical formulae shown in figures), chlorocarbonate phase (C1: $Mg(OH)_2$-$MgCl_2$-$2MgCO_3$-$6H_2O$), and magnesium chloride salt 5-phase (H5: $5Mg(OH)_2$-$MgCl_2$-$8H_2O$). These products confirm the occurrence of MgO carbonation and chemical interactions within the MgO-$MgCl_2$-H_2O ternary system in the soil matrix.

Fig. 8(a) illustrates the influence of $MgCl_2$ content on chemical product formation at a constant initial water content of 30%. Comparative analysis demonstrates that increased $MgCl_2$ content resulted in reduced XRD peak intensity for $Mg(OH)_2$, while simultaneously enhancing peak signatures for the chlorocarbonate phase and magnesium carbonate trihydrate. This phenomenon can be attributed to $Mg(OH)_2$ consumption during the formation of these secondary products. The chlorocarbonate phase primarily originates from the carbonation of 3-phase compounds ($3Mg(OH)_2$-$MgCl_2$-$8H_2O$) as described by Eq. (10), while dynamic interconversion between metastable 5-phase and 3-phase compounds may occur.

$$3Mg(OH)_2\cdot MgCl_2\cdot 8H_2O+CO_2\rightarrow Mg(OH)_2\cdot MgCl_2\cdot 2MgCO_3\cdot 6H_2O+2H_2O \quad (10)$$

Fig. 8(b) demonstrates the impact of initial water content on XRD patterns at 12% $MgCl_2$ content. The chlorocarbonate phase and magnesium carbonate trihydrate show progressive reduction with increasing water content. Notably, distinct 5-phase products are observed in specimens with 35% initial water content, whereas these phases diminish or disappear at lower moisture levels. This behavior stems from three primary factors: 1) elevated pH in high-water-content specimens enhances 5-phase stability, 2) high $MgCl_2$ concentrations promote 5-phase formation followed by gradual conversion to 3-phase during carbonation (Eq. (10)), and 3) excessive water content impedes CO_2 diffusion, thereby limiting chlorocarbonate and trihydrate formation. The correlation between XRD peak intensities of these crystalline phases and strength evolution suggests their crucial role in mechanical property development.

3.3.2 Thermogravimetry/derivative thermogravimetry (TG/TGD)

Thermogravimetric analysis results under varying initial water and $MgCl_2$ contents are presented in Fig. 9. The TG curves reveal temperature-dependent mass loss progression, with minimum mass loss (6% $MgCl_2$, 30% water) and maximum mass loss (12% $MgCl_2$, 25% water) specimens showing distinct thermal behaviors. DTG curves exhibit three characteristic peaks centered near 100°C, 184°C, and 395-450°C, corresponding sequentially to crystallization water loss,

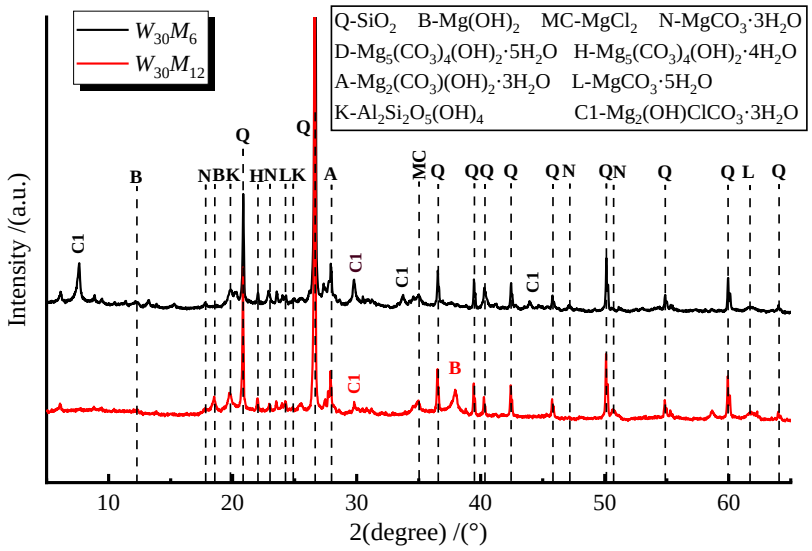

(a) The effect of $MgCl_2$ content

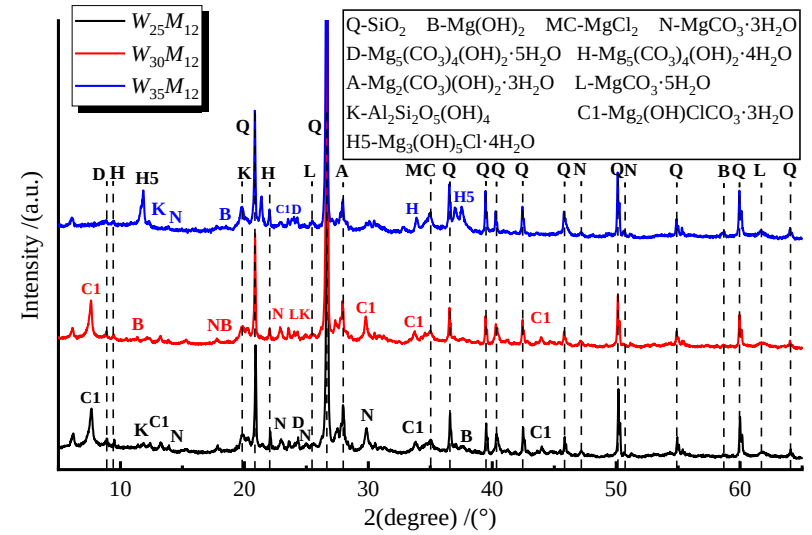

(b) The effect of initial moisture content

Fig. 8 XRD diagram of carbonated samples under different conditions

bound water removal, and $Mg(OH)_2$ dehydroxylation. The peak integration areas show proportional relationships with mass changes observed in TG curves.

As detailed in Table 6, specimens with 30% water content and 6% $MgCl_2$ displayed minimal crystallization water loss, indicating the limited formation of hydration and carbonation products. Conversely, the 25% water content or 12% $MgCl_2$ combination shows maximum $Mg(OH)_2$ decomposition (4.21% mass loss), reflecting a substantial generation of magnesium carbonates. These thermal decomposition patterns align with the previously discussed strength development mechanisms.

3.3.3 Microstructure

Fig. 10 presents ×1500 magnified SEM images of carbonated specimens under different $MgCl_2$ and water content conditions. The XRD pattern shows the generation of a large number of magnesium carbonate crystals, indicating that CO_2 curing effectively promotes the formation of cementitious products (Liu *et al.* 2023), further explaining the mechanism of strength growth. Chau *et al.*'s study showed that the chlorocarbonate phase crystals were curved short rods and the 5-phase crystals were needle-like structures (Chau et al. 2008). At 6% $MgCl_2$, specimens exhibited porous structures with limited spherical carbonation products and abundant flocculent $Mg(OH)_2$, resulting in poor particle cementation (Figs. 10(a), 10(c) and 10(e)). In contrast, 12% $MgCl_2$ specimens displayed dense matrices containing needle-like 5-phase crystals, prismatic magnesium carbonate trihydrate, and curved chlorocarbonate phase rods (Figs. 10(b), 10(d) and 10(f)). The 5-phase crystals primarily occupied pore spaces, while the trihydrate and chlorocarbonate phases formed surface coatings,

Table 6 Mass loss of carbonated/solidified soil at every stage (%)

Temperature range	$W_{30}M_3$	$W_{30}M_6$	$W_{30}M_{12}$	$W_{25}M_{12}$	$W_{35}M_{12}$
Crystalline water (50~130℃)	5.95	3.03	3.93	5.6	7.32
Bound water (140~200℃)	2.61	1.26	3.22	3.55	3.41
Dehydroxylation (350~450℃)	9.49	5.9	8.28	9.86	5.78

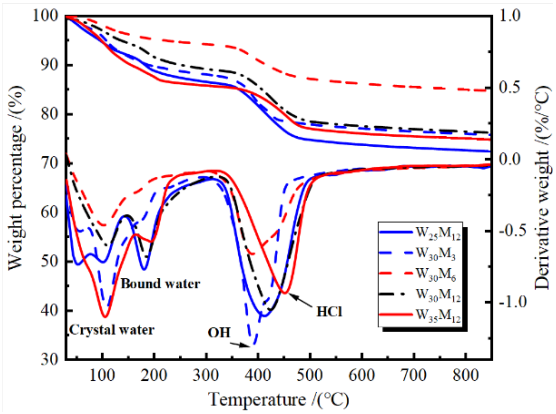

Fig. 9 TG-DTG curve under different salt content and water content

creating an interwoven network of carbonation/hydration products that enhanced particle bonding and pore filling. Similar phase transitions have been observed in alkali-activated materials, further confirming the role of MgO in governing carbonate polymorphism (Gholami *et al*. 2024). Comparative analysis across water contents reveals distinct microstructural configurations: 25-35% of water content specimens predominantly contain chlorocarbonate and 5-phase crystals, while 30% of water content specimens show trihydrate crystal dominance. This trihydrate prevalence at optimal moisture conditions corresponds to maximum strength improvement through effective particle cementation.

3.4 Water-immersion durability

Fig. 11 illustrates the unconfined compressive strength variations of specimens under different water immersion durations. As shown in the figure, all specimens exhibit progressive strength reduction with prolonged water exposure. Notably, specimens containing 3% and 6% $MgCl_2$ demonstrated significant particle detachment and structural disintegration upon immersion, rendering strength measurement unfeasible. The strength degradation pattern reveals an inverse relationship with $MgCl_2$ concentration, following the order: 12% > 9% > 0% $MgCl_2$ content. Specifically, specimens maintained relatively stable strength values during the initial 7-day immersion period, followed by a marked decline to 0-2 MPa after 14 days of water exposure. This behavior can be attributed to distinct chemical mechanisms: (1) the 12% $MgCl_2$ specimens primarily undergo hydration reactions, exhibiting poor water-immersion durability that accelerates strength deterioration; (2) the salt-free specimens rely solely on

(a) $W_{25}M_6$

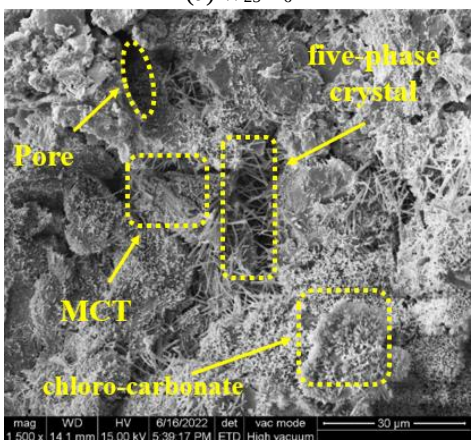

(b) $W_{25}M_{12}$

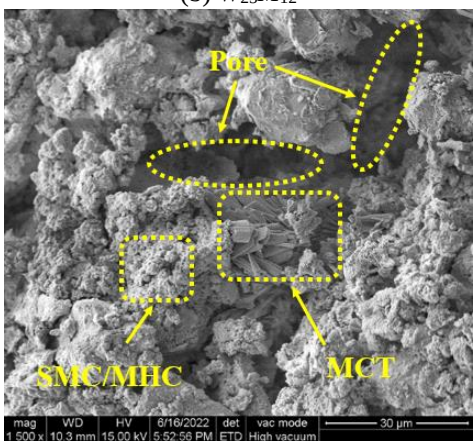

(c) $W_{30}M_6$

Fig. 10 SEM images of typical carbonated samples (×1500); SMC/MHC: spherical magnesium carbonate/magnesium hydrocarbon; MCT: magnesium trihydrate

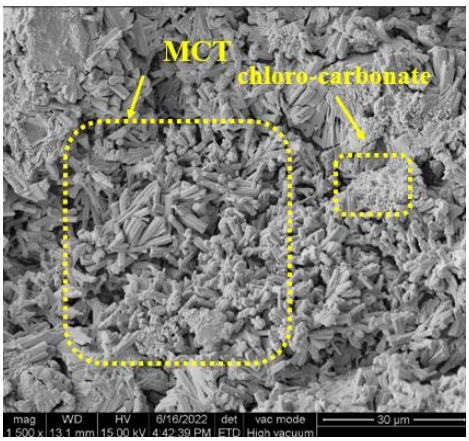

(d) $W_{30}M_{12}$

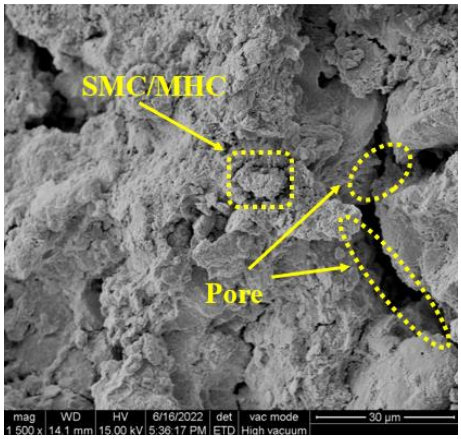

(e) $W_{35}M_6$

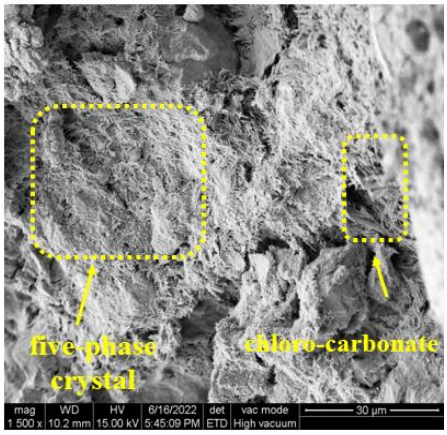

(f) $W_{35}M_{12}$

Fig. 10 Continued-

carbonation processes, though their strength reduction stems from the inherent water sensitivity of pulverized clay; (3) lower $MgCl_2$ concentrations (3-6%) promotes more pronounced carbonation effects, but suffers combined swelling mechanisms (hydration expansion and salt crystallization) that compromised structural integrity; and (4) optimal performance occurs at 9% $MgCl_2$ content, where the balanced carbonation-hydration interactions minimize post-immersion strength loss.

These findings suggest that carbonation treatment effectively addresses swelling issues in chlorinated silty or sandy soils across various $MgCl_2$ concentrations, while simultaneously enhancing water-immersion durability. The 9% $MgCl_2$ concentration represents a critical threshold for achieving optimal equilibrium between competing chemical processes.

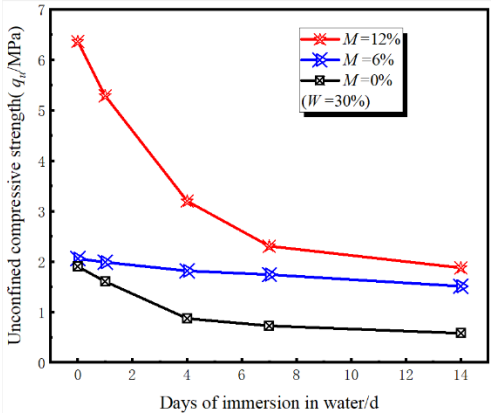

Fig. 11 Unconfined compressive strength of carbonated specimens after water immersion

4. Discussion

To systematically investigate the influence of MgO-$MgCl_2$-H_2O ratios on the mechanical performance of carbonated specimens, this study analyzed the relationships between compressive strength and two critical parameters of the magnesium-to-chlorine molar ratio (R_M) and the water-to-chlorine molar ratio (R_H). These ratios were derived through stoichiometric calculations (Eqs. (11) and (12))

$$R_M = \frac{n_{MgO}}{n_{MgCl_2}} = \frac{m_{MgO} / M_{MgO}}{m_{MgCl_2} / M_{MgCl_2}} = \frac{19 \cdot m_{MgO}}{8 \cdot m_{MgCl_2}} \quad (11)$$

$$R_H = \frac{n_{H_2O}}{n_{MgCl_2}} = \frac{m_{H_2O} / M_{H_2O}}{m_{MgCl_2} / M_{MgCl_2}} = \frac{95 \cdot m_{H_2O}}{18 \cdot m_{MgCl_2}} \quad (12)$$

where n_{MgO}, n_{MgCl_2} and n_{H_2O} represent the molar quantities of reactive MgO, $MgCl_2$, and H_2O, respectively; m_{MgO}, m_{MgCl_2} and m_{H_2O} denote their corresponding mass (g); and their molar masses of $M_{MgO} = 40$ g/mol, $M_{MgCl_2} = 95$ g/mol and $M_{H_2O} = 18$ g/mol are utilized for practical formulation design.

Fig. 12 illustrates the strength evolution of carbonated specimens with varying R_M under different initial moisture conditions. A rapid decline in strength occurs as R_M increases from 3 to 6, followed by plateauing as R_M ranges from 6 to 12. This two-phase behavior suggests that water content critically governs strength development in low R_M ranges (R_M <6), while its influence diminishes at higher R_M values. This nonlinear response also highlights the critical influence of MgO dosage optimization in balancing reaction kinetics and final product formation.

Conversely, Fig. 13 demonstrates the strength variation of carbonated samples with the water-chlorine ratio R_H. The strength decreases exponentially with increasing R_H across

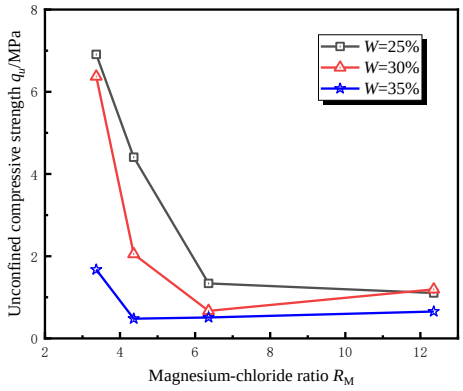

Fig. 12 Unconfined compressive strength under different magnesium-chloride ratio

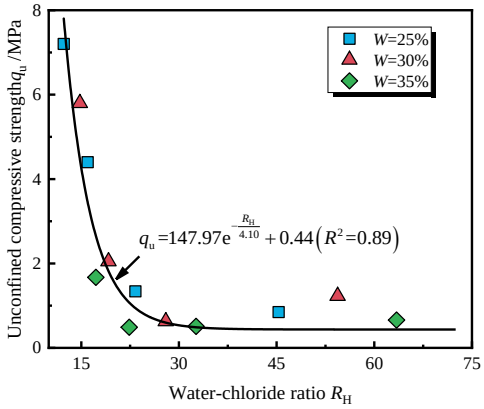

Fig. 13 Unconfined compressive strength under different water-chloride ratio

the tested range (R_H=12–65), and the relationship between strength and R_H is well-characterized by the empirical model in Eq. (13). Notably, optimal strength is achieved at R_H=12–17. This deterioration correlates with excessive water content diluting the cementitious matrix and creating discontinuous pore structures, consistent with nucleation theory in cement chemistry.

$$q_u = 147.97e^{-\frac{R_H}{4.1}} + 0.44 (R^2 = 0.89) \quad (13)$$

The findings collectively highlight the pivotal roles of *M* and *H* in governing the carbonation efficacy of MgO-$MgCl_2$-treated chloride-rich soils. Strength maximization occurs at R_M=3–6 and R_H=12–17, aligning with previous research by Ba and Guan (2009), who identified R_M <6 and R_H =12–18 as favorable ranges for the hydration of magnesium chloride cement. This consistency underscores the universal importance of stoichiometric balance in MgO-$MgCl_2$ systems. The mechanistic basis lies in the dual role of R_H: (1) facilitating Mg^{2+} and Cl^- ion dissociation at moderate levels; and (2) enabling complete carbonation through controlled water availability. Further analysis reveals a critical trade-off: lower R_M values (R_M <6) enhance strength but compromise water stability due to incomplete reaction phases, while higher R_M (R_M >6) improves durability at the expense of mechanical performance. This dichotomy necessitates a balanced optimization of R_M and R_H to concurrently achieve high strength and long-term stability.

From an application perspective, these findings advance two practical solutions for chloride-rich soil treatment: (1) the direct carbonation of MgO-$MgCl_2$ stabilized soils, leveraging controlled reaction conditions; and (2) in-situ enhancement of existing $MgCl_2$-containing foundations through optimized MgO carbonation. Both approaches effectively mitigate chloride-induced swelling while improving load-bearing capacity, demonstrating significant potential for infrastructure projects in saline-alkali regions. Further field validation should focus on muti-objective long-term performance under such cyclic wet-dry conditions.

This study has unveiled the mechanism of mechanical property optimization and the law of microscopic phase transformation for MgO-$MgCl_2$ carbonated solidified saline soft soil through a series of systematic experiments. The major contributions are as follows:

- The synergistic effect of $MgCl_2$ content and initial moisture content on carbonation efficiency has been clarified;
- The formation mechanism of the chlorocarbonate phase ($Mg_2CO_3(OH)Cl{\cdot}3H_2O$) and the 5-phase crystal ($5Mg(OH)_2{\cdot}MgCl_2{\cdot}8H_2O$) has been elucidated, revealing that the dense microstructure is the fundamental cause of strength enhancement;
- A quantitative optimization model for the magnesium-chlorine ratio and water-chlorine ratio has been established, offering design parameters for low-carbon improvement of saline soils.

In recent years, composite new materials have emerged a new trend in the solidification treatment of special soil. For instance, Mustafayeva et al. showed that industrial by-products, such as alkaline oxygen furnace (BOF) slag, hold potential for stabilizing expansive soils (Mustafayeva *et al.* 2024). Rauf *et al.* investigated alternative binders like calcium sulfoaluminate (CSA) cement and found that it exhibits remarkable resistance to cyclic wet- dry conditions, with higher cement content reducing strength loss (Rauf *et al.* 2025). However, traditional cement - based stabilization technologies for saline soils have notable limitations. To address this, some researchers have proposed innovative ideas using nanomaterials, such as multi - walled carbon nanotubes (Ahmadi *et al.* 2024), which significantly enhance landslide resistance by improving soil shear strength and permeability control.

Based on the limitations of this study and the research trend of green new curing materials, future research could focus on the following directions:

- Conduct research on the solidification and carbonation of various materials, and establish a classified optimization model;
- Perform long-term performance evaluations, conducting accelerated aging tests (such as dry-wet cycles, UV irradiation, etc.), and quantify the stability and lifespan prediction of carbide products;
- Explore innovative solidification processes, including not only the combination of solidification materials and chemical methods but also material reinforcement

for foundation construction, such as piles and anchor rods in engineering.

5. Conclusions

This study systematically investigated the physicochemical, mechanical properties, and microstructural evolution of MgO-$MgCl_2$ carbonated soil through comprehensive macro-microscopic analyses, with a particular focus on the effects of $MgCl_2$ content and initial water content. The principal findings can be summarized as follows:

- Both strength and modulus exhibited an inverse relationship with initial water content while showing an initial gradual enhancement followed by substantial improvement, with minimum values observed at 3-6% $MgCl_2$. The modulus showed a proportional relationship with strength with a slope of 14 to 75.
- Carbon absorption efficiency ranged between 10%~40%. Pre- and post-carbonation demonstrated a progressive decline with increasing $MgCl_2$, though hygroscopic effects in the carbonation environment elevated moisture retention in $MgCl_2$-containing samples. The pH evolution revealed a decreasing trend with higher $MgCl_2$ content, with the reduction of post-carbonation pH being less pronounced compared to pre-carbonation states. The pH showed positive a correlation with initial water content.
- Microscopic analysis shows that in the system with low $MgCl_2$ content (6%), the main components are flocculent $Mg(OH)_2$ and loose carbonation products, which exhibit poor bonding properties. In contrast, under high $MgCl_2$ content (12%) conditions, needle shaped 5-phase crystals ($5Mg(OH)_2 \cdot MgCl_2 \cdot 8H_2O$) and short rod-shaped chlorocarbonate phases ($Mg_2CO_3(OH)Cl \cdot 3H_2O$) form a dense interwoven structure. The structure enhances pore filling and serves as the core mechanism for the strength increase. The XRD and TG/DTG results further confirm that the proportion of carbide products is positively correlated with mechanical properties.

Through quantitative analysis of the magnesium-chloride ratio (R_M) and water-chloride ratio (R_H), the optimal reaction range was determined to be R_M<6 and R_H=12-17 (corresponding to a moisture content≤30% and $MgCl_2$ content≥6%). This combination of parameters can balance carbonation and hydration reactions, taking into account short-term strength and water--immersion durability. It represents the optimal initial condition for the strength development of MgO-$MgCl_2$ carbon fixed foundation soil.

Acknowledgments

The authors would like to thank the financial support of the National Natural Science Foundation of China (42477163, 41902286), the Open Research Program of Key Laboratory of Port Geotechnical Engineering in the Ministry of Communications (2024-11-088-0114), the CRSRI Open Research Program (CKWV20221015/KY), Technology development Project from Yellow River Engineering Consulting Co., LTD (2023KY031(2)), and Jiangsu Provincial Transportation Engineering Construction Bureau (2023-15).

References

Ahmadi H, Satyanaga A, Orazayeva S., Kalimuldina, G., Rahardjo, H., Qian, Z. and Kim, J. (2024), "Carbon nanotubes for slope stabilization of silty soil", *Infrastructure*s, **9**(12), 232. https://doi.org/10.3390/infrastructures9120232.

Aye, T. and Oguchi, C.T. (2011), "Resistance of plain and blended cement mortars exposed to severe sulfate attacks", *Constr. Build. Mater*., **256**(1), 2988-2996. https://doi.org/10.1016/j.conbuildmat.2010.11.106.

Ba, H.J. and Guan, H. (2009), "Influence of MgO/$MgCl_2$ molar ratio on phase stability of magnesium oxychloride cement", *J. Wuhan Univ. Technology-Materials Sci. Edition*, **24**(3), 476-481. https://doi.org/10.1007/s11595-009-3476-3.

Ban, R.L., Zha, F.S., Kang, B., Wu, S., Song, Y. and Chen, H. (2024), "Mechanisms of enhancing MgO for stabilization/solidification of Pb-contaminated red clay through CO_2 sequestration", *J. Environ. Management*, **366**, 121810. https://doi.org/10.1016/j.jenvman.2024.121810.

Cai, G.H., Liu, S.H., Du, Y.J., Zhang, D. and Zheng, X. (2015), "Strength and deformation characteristics of carbonated reactive magnesia treated silt soil", *J. Central South Univ*., **22**(5), 1859-1868. https://doi.org/10.1007/s11771-015-2705-5.

Cai, G.H., Liu, S.Y. and Cao, J.J. (2017), "The effect of initial moisture content on the strength and resistivity of MgO carbonated silt", *J. China Highway Eng*., **30**(11), 18-26. https://doi.org/10.19721/j.cnki.1001-7372.2017.11.003.

Cai, G.H., Liu, S.Y., Du, G.Y., Wang, L., Li, J.S. and Liu, L. (2020), "Hydraulic conductivity characteristics of carbonated reactive magnesia-treated silt", *Bull. Eng. Geol. Environ*., **79**, 3033-3047. https://doi.org/10.1007/s10064-020-01746-6.

Chau, C.K. and Li, Z. (2008), "Microstructures of magnesium oxychloride", *Mater. Struct*., **41**(5), 853-862. https://doi.org/10.1617/s11527-007-9289-y.

Gao, J.B. and Yu, Y.G. (2011), "Research progress in engineering and mechanical properties of the saline soil", *Mech. Eng*., **33**(4), 1.

Gholami, S., Kim, Y.R., Little, D., Kwon, S. and Jung, J.S. (2024), "Carbonation of one-part alkali-activated materials incorporated by MgO: phase characteristics and micromechanical properties", *Constr. Build. Mater*., **441**, 137400. https://doi.org/10.1016/j.conbuildmat.2024.137400.

Góchez, R., Vreeland, T., Wambaugh, J. and Kitchens, C.L. (2017), "Conversion of magnesium oxychloride to chlorartinite and resulting increased water resistance", *Mater. Lett*., **207**, 1-3. https://doi.org/10.1016/j.matlet.2017.06.124.

He, P., Poon, C.S. and Tsang, D.C.W. (2017), "Using incinerated sewage sludge ash to improve the water resistance of magnesium oxychloride cement (MOC)", *Constr. Build. Mater*., **147**, 519-524. https://doi.org/10.1016/j.conbuildmat.2017.04.187.

Huang, Q., Zheng, W.X., Xiao, X.Y., Dong, J., Wen, J. and Chang, C. (2022), "A study on the salt attack performance of magnesium oxychloride cement in different salt environments", *Constr. Build. Mater*., **320**, 126224. https://doi.org/10.1016/j.conbuildmat.2021.126224.

Jun, Y., Han, S.H. and Kim, J.H. (2024), "Performance of CO_2-cured alkali-activated blast-furnace slag incorporating

magnesium oxide", *Constr. Build. Mater.*, **429**, 136462. https://doi.org/10.1016/j.conbuildmat.2024.136462.

Karimi, Y. and Monshi, A. (2011), "Effect of magnesium chloride concentrations on the properties of magnesium oxychloride cement for nano SiC composite purposes", *Ceramics Int.*, **37**(7), 2405-2410. https://doi.org/10.1016/j.ceramint.2011.05.082.

Li, B.Z., Min, F.L., Zhou, X., Zhang, N., Wang, X. and Yao, Z. (2024), "Strength characteristics and solidification carbonization mechanism of MgO-based shield tunneling centrifugal waste silt", *Constr. Build. Mater.*, **447**, 138132. https://doi.org/10.1016/j.conbuildmat.2024.138132.

Li, Y. (2016), "The geochemical characteristics and environmental significance of soil and its red clay layer in the Yellow River Delta", Ph.D. Dissertation, Yantai Institute of Coastal Zone, Chinese Academy of Sciences, Yantai.

Li, Z., Qian, J.S., Qin, J.H., Hua, Y., Yue, Y. and Tang, H. (2023), "Cementitious and hardening properties of magnesia (MgO) under ambient curing conditions", *Cement Concrete Res.*, **170**, 107184. https://doi.org/10.1016/j.cemconres.2023.107184.

Liu, L. and Wang, B. (2021), "Protection of halophytes and their uses for cultivation of saline-alkali soil in China", *Biology*, **10**(5), 353. https://doi.org/10.3390/biology10050353.

Liu, W.H., Hong, G.Q., Li, W.G., Zhang, Y. and Sun, Y. (2023), "Influence of initial moisture and reactive MgO content on mechanical and microstructural characteristics of carbonated reactive magnesia treated soft clay", *KSCE J. Civil Eng.*, **27**(5), 2004-2015. https://doi.org/10.1007/s12205-023-1668-6.

Liu, Z.Z., Balonis, M., Huang, J., Sha, A. and Sant, G. (2017), "The influence of composition and temperature on hydrated phase assemblages in magnesium oxychloride cements", *J. Am. Ceramic Soc.*, **100**(7), 3246-3261. https://doi.org/10.1111/jace.14817.

Ma, J.L., Zhao, Y.C., Wang, J.M. and Wang, L. (2010), "Effect of magnesium oxychloride cement on stabilization/solidification of sewage sludge", *Constr. Build. Mater.*, **24**(1), 79-83. https://doi.org/10.1016/j.conbuildmat.2009.08.011.

Miller, S.A. and Moore, F.C. (2020), "Climate and health damages from global concrete production", *Nat. Climate Change*, **10**(5), 439-443. https://doi.org/10.1038/s41558-020-0733-0.

Mustafayeva, A., Moon, S.W., Satyanaga, A. and Kim, J. (2024), "Enhancing mechanical properties of expansive soil through BOF slag stabilization: A sustainable alternative to conventional methods", *Minerals*, **14**(11), 1145. https://doi.org/10.3390/min14111145

Onyekwena, C.C., Xue, Q., Li, Q., Umeobi, H.I., Ghaffar, A. and Fasihnikoutalab, M.H. (2023), "Advances in the carbonation of MgO-based binder and CO_2 utilization in the construction industry", *Clean Technol. Environ. Policy*, **25**(6), 1763-1782. https://doi.org/10.1007/s10098-023-02482-7.

Rauf, A., Moon, S.W., Satyanaga, A. and Kim, J. (2025), "Assessing durability and stability of calcium sulfoaluminate cement-stabilized soils under cyclic wet–dry conditions", *Buildings*, **15**(2), 228. https://doi.org/10.3390/buildings15020228.

Sagidullina, N., Satyanaga, A., Kim, J. and Moon, S.W. (2025), "Engineering behavior and geotechnical challenges of sulfate-rich soils in Astana", *Front. Built Environ.*, **10**, 1504643. https://doi.org/10.3389/fbuil.2024.1504643.

Seo, J., Park, S., Kim, G.M. and Park, S. (2024), "Exploring natural and accelerated carbonation of alkali-activated slag", *Constr. Build. Mater.*, **432**, 136459. https://doi.org/10.1016/j.conbuildmat.2024.136459.

Sun, J., Chen, H.J., Wang, S.H. and Li, H.M. (2014), "Case study on soft foundation of coastal saline soil", *Adv. Mater. Res.*, **1065-1069**, 469-474. https://doi.org/10.4028/www.scientific.net/AMR.10651069.469.

Sun, Y., Liu, W.H., Li, W.G., *et al.* (2023), "Experimental study on mechanical properties and microscopic mechanism of magnesium oxychloride cement solidified sludge", *J. Dalian Univ. Technol.*, **63**(3), 313-320. https://doi.org/10.7511/dllgxb202303011.

Walling, S.A. and Provis, J.L. (2016), "Magnesia-based cements: a journey of 150 years, and cements for the future", *Chem. Rev.*, **116**(7), 4170-4204. https://doi.org/10.1021/acs.chemrev.5b00463.

Wan, Q. (2022), "Research on deformation characteristics of coarse grain chlorine saline soil roadbed in high cold salt lake area under traffic load", Dissertation, Xi'an: Chang'an University. https://doi.org/10.26976/d.cnki.gchau.2022.000101.

Wang, D.X., Zhu, J.Y. and He, F.J. (2019), "CO_2 carbonation-induced improvement in strength and microstructure of reactive MgO-CaO-fly ash-solidified soils", *Constr. Build. Mater.*, **229**, 116914. https://doi.org/10.1016/j.conbuildmat.2019.116914.

Wang, Z., Park, S., Khalid, H.R., Kim, S. and Lee, H.K. (2024), "Carbonation behavior of aged alkali-activated fly ash/slag binder modified by MgO with different reactivities", *Mater. Struct.*, **57**(5), 119. https://doi.org/10.1617/s11527-024-02397-9.

Yang, X.F., You, Z.M., Niu, F.J., *et al*. (2014), "Research progress on the solidification effect of solidification agents on the physical and mechanical properties of saline soil", *Glaciology Geocryology*, **36**(2), 376-385. https://doi.org/10.7522/j.issn.1000-0240.2014.0046.

Yi, L., Liska, M., Unluer, C. and Al-Tabbaa, A. (2013), "Carbonating magnesia for soil stabilization", *Can. Geotech. J.*, **50**(8), 899-905. https://doi.org/10.1139/cgj-2012-0364.

Yu, H. (2004), "Durability, mechanism, and service life prediction method of high-performance concrete in salt lake areas", Dissertation, Nanjing: Southeast University.

Zhang, D.W., Cao, Z.G., Fan, L.B., Kiu, S. and Liu, W. (2014), "Evaluation of the influence of salt concentration on cement stabilized clay by electrical resistivity measurement method", *Eng. Geol.*, **170**, 80-88. https://doi.org/10.1016/j.enggeo.2013.12.010.

Zhao, G.W., Shi, M., Fan, H.H., Cui, J. and Xie, F. (2020), "The influence of multiple combined chemical attack on cast-in-situ concrete: deformation, mechanical development and mechanisms", *Constr. Build. Mater.*, **251**, 118988. https://doi.org/10.1016/j.conbuildmat.2020.118988.

Zhong, Y.Q., Cai, G.H., Wang, S.Q., Qin, H., Zhang, C. and Li, J. (2022), "Influence of organic content on the mechanical properties of organic-rich soils stabilized with CaO-GGBS binder and PC", *Water*, **14**(19), 3053. https://doi.org/10.3390/w14193053.

JS